Smart Manufacturing in Rolling Process Based on Thermal Safety Monitoring by Fiber Optics Sensors Equipping Mill Bearings

applied sciences

MDPI

Article

Smart Manufacturing in Rolling Process Based on Thermal Safety Monitoring by Fiber Optics Sensors Equipping Mill Bearings

Eugenio Brusa *, Cristiana Delprete and Lorenzo Giorio

Department of Mechanical and Aerospace Engineering, Politecnico di Torino, 10129 Torino, Italy; cristiana.delprete@polito.it (C.D.); lorenzo.giorio@polito.it (L.G.)
* Correspondence: eugenio.brusa@polito.it; Tel.: +39-0110906730 or +39-0110906895

Abstract: The steel rolling process is critical for safety and maintenance because of loading and thermal operating conditions. Machinery condition monitoring (MCM) increases the system's safety, preventing the risk of fire, failure, and rupture. Equipping the mill bearings with sensors allows monitoring of the system in service and controls the heating of mill components. Fiber optic sensors detect loading condition, vibration, and irregular heating. In several systems, access to machinery is rather limited. Therefore, this paper preliminarily investigates how fiber optics can be effectively embedded within the mill cage to set up a smart manufacturing system. The fiber Bragg gratings (FBG) technology allows embedding sensors inside the pins of backup bearings and performing some prognosis and diagnosis activities. The study starts from the rolling mill layout and defines its accessibility, considering some real industrial cases. Testing of an FBG sensor prototype checks thermal monitoring capability inside a closed cavity, obtained on the surface of either the fixed pin of the backup bearing or the stator surrounding the outer ring. Results encourage the development of the whole prototype of the MCM system to be tested on a real mill cage in full operation.

Keywords: FBG sensors; smart bearing; structural mechatronics; smart manufacturing; industry 4.0

Citation: Brusa, E.; Delprete, C.; Giorio, L. Smart Manufacturing in Rolling Process Based on Thermal Safety Monitoring by Fiber Optics Sensors Equipping Mill Bearings. *Appl. Sci.* **2022**, *12*, 4186. https://doi.org/10.3390/app12094186

Academic Editor: Valentin L. Popov

Received: 16 March 2022
Accepted: 19 April 2022
Published: 21 April 2022

1. Introduction

The steelmaking process looks critical for energy consumption, power losses, environmental pollution, and the safety of human operators [1]. The hot rolling mill exploits a huge amount of energy, while in cold rolling are even critical vibration, friction, and chattering [2]. Moreover, the risk of fire, due to anomalous heating of mill components and lubricant, makes the system design rather difficult.

Nowadays, the enabling technologies of smart manufacturing allow mitigating those problems [3]. They help in reducing mill vibration and material friction, to make higher the product quality, control the state of lubricant and temperature, and even save energy in terms of heat, vibration, and water flow control when it is used to keep the temperature of roll surface as low as possible. Moreover, early detection of failures and damages allows for applying effective predictive maintenance.

A distributed monitoring system with capillary access to the most hidden parts of the mill cage may operate those actions and prevent failures. It warns operators about any incipient faults [4] but even collects data from the machine elements [5]. It usually exploits a network of distributed sensors, although some machine components, such as bearings, may play the role of physical nodes of the network, to monitor the whole machinery when they embed transducers [6,7]. Particularly, mechanical bearings are referred to as "smart" when sensors monitor "in situ" the overall system behavior [8,9]. They constitute a node of the distributed monitoring system to enhance the mill connectivity for monitoring, diagnosis, and prognosis purposes, leading to "machinery condition monitoring" (MCM) [10,11]. Some network services provided by the Internet of Things (IoT) assure that connectivity [12].

In the literature, wide use of smart bearings to detect vibration, noise, and resonances is proposed [13], but a relevant part of MCM for safety belongs to the early detection of temperature changes, especially in the most hidden elements of the rolling mill.

This paper investigates the specific use of smart bearing to detect any anomalous heating in the rolling mill, through the fiber optics sensors, by monitoring elements of the mill cage, being deeply embedded and poorly accessible. The mill system architecture is analyzed. The study proposes access to backup bearings through their supporting and fixed pins or through the structure of the mill cage, constraining the bearing rings. This choice depends on the mill layout and its operation in either cold or hot rolling processes. The investigation then identifies the fiber path inside the rolling mill and sets up the interface to the bearing ring.

A preliminary experimental validation demonstrates the effectiveness of the fiber Bragg gratings (FBG) [14] when embedded inside the mill system. An assessment of sensors specifications includes a preliminary investigation of the fluidic interface exploited to help the measurement in operation by considering the availability of water and lubricant oil, respectively, in the mill cage. This preliminary investigation encourages finalizing the design assessment of this approach for industrial application and for the proposed implementation of artificial intelligence packages.

2. Materials and Methods

To proceed in the proposed design activity, a first investigation explores the smart bearing technology, defines the most relevant requirements to be fulfilled, and selects the most useful technological approach. A second step concerns the analysis of the rolling mill layout to identify the operational goals and architectural accesses available for the monitoring system. The focus then moves to the selected fiber optics to identify their properties and some main design parameters. Finally, a preliminary definition of the system architecture is proposed. A validation of this study follows and analyses the performance into a small test bed of FBG sensors to identify some design issues and potential obstacles and to test the system performance. This activity leads to discussing some preliminary results.

2.1. The Smart Bearing Technology and Its Application to Rolling Process

The goal of smart bearing is to detect any abnormal operation of the rolling mill ("out-monitoring") as well as early identification of any inner faults ("in-monitoring"). In the steelmaking process, the risk of catastrophic events motivates equipping all the machinery with an effective condition monitoring system. This is carried out, for instance, for the electric arc furnace [15]. In rotating machinery, statistics demonstrate that several faults rise up in bearings, and effective condition monitoring can detect their immediate consequences and evidence. A fault there nucleated affects the rotor shaft dynamics and its stability [16–18]. Therefore, monitoring bearings allows for assessing the overall system health and reliability. The smart bearing needs to be power supplied, either autonomously or through a light and flexible wire connection, and suitably miniaturized to be embedded into the machine [19]. Embedding sensors in some systems is rather difficult, but providing a condition monitoring of the rolling mill promotes the automation of steel production through some mechatronic manufacturing systems [20–22]. Some obstacles to wireless telecommunication in the rolling mill actually exist. Therefore, a deep research activity promotes the development of effective sensor technologies.

Since the beginning of this millennium [23], several solutions have been proposed. Kovacs [24] exploits a wireless and temperature-sensitive capacitor sensor (up to 220 °C), being more effective than thermocouples. Draney [25] introduces an autonomous smart bearing suitable for harsh environments being able to operate up to 300 °C and harvest thermal energy from the environment through a thermoelectric generator (TEG), even used in some other applications [26]. It exploits wireless communication to send data. In the work of [9], a multi-tasking smart bearing is proposed, including two piezoelectric

vibration sensors, two magneto-electric speed sensors, and two thermocouples. In the work of [27], the whole sensing unit is designed. A sensor based on a microprocessor monitors the bearing duty cycles and dynamics. Vibration data in two directions are collected and preliminarily analyzed. This system sends the monitoring system directly the evidence of fault detection, in either the shaft or bearings, resorting to the wavelet energy spectrum technique. In the work of [28], a small strain gauge, for high spatial resolution and low response time, is applied to rolling contact in the axial roller bearing. A comprehensive review of the state of the art of the smart bearing technologies and the structure of integrated sensors and of the parameters to be monitored for the aircraft engine is depicted in the work of [29]. Choi introduces [30] a cost-effective triboelectric sensor embedded into a roller bearing based on the triboelectric effect. Zhang [31] proposes a review of the most recent smart bearing layouts and focuses on some key issues such as signal detection, power supply, read-out circuits, and bearing arrangement. Zaghari [32] presents an integrated and self-powered wireless system for high-temperature (above 125 °C) environments powered by a thermoelectric generator for bearing condition monitoring in aircraft application, where the TEG allows collecting data every 46 s and transmitting every 260 s. Brusa [19] designed an autonomous configuration based on a vibration energy harvester. The energy conversion exploits vibration of a flexible structure, with surface-bonded piezoelectric layers, being excited by some permanent magnets during their rotation. All the above-mentioned solutions exploit quite suitable access to the monitored system. The ratio between the size of the sensor and of the machine element is never too low, and environmental conditions are only seldom critical. In case of the rolling mill, those benefits are very often absent, and a specific strategy is required.

2.2. The Rolling Mill Architecture and Main Customer Needs

The rolling mill performs either hot or cold material processing, exploiting different architectures [33,34]. In the hot rolling of steel, the billet is heated approximately up to 900 °C, and then it passes through the rolls of the rolling path. This action allows reducing its thickness in every step of rolling, namely "pass", with a given surface finish of the rolled product. Moreover, heating and cooling of the rolled material even cause some geometrical imperfections in the final product. Their prediction allows for assessing the mill layout and choosing the most suitable manufacturing technology. In the hot rolling mill, the working roll in contact with the worked material undergoes a very high temperature, which requires an adequate cooling action, being provided by water injection, on the roll surface. Unfortunately, the roll is exposed to several thermal shocks per revolution, leading to surface cracking and spalling damages [35]. Those effects increase the severity of the wear process and sometimes excite the thermomechanical fatigue of materials [36], thus reducing the life of the working roll and even the mean time between failures, or MTBF [37]. If the mean temperature of the roll reaches a defined threshold value, some collateral risks increase, such as those of combustion of lubricant and of unsafe interaction with human operators. Those effects motivate thermal monitoring of the rolling mill elements.

In contrast, the cold rolling process offers several advantages. It provides a more accurate shape of the final product and a smoother and better surface finish. Among several mill configurations, the Sendzimir mill (Figure 1a) is often exploited for fast material processing [38]. It includes slender working rolls in contact with rolled material, surrounded by several back rolls, used to prevent bending and vibration of the work roll to ensure precise processing and reduce surface defects. A more compact layout of the cluster mill characterizes the Z-Mill [39], where the crown of back rolls is limited to a few elements, actively controlled by hydraulic actuators, which allow applying the required forces to control the work roll deformation [2]. This layout leads to a reduced size of the rolling mill, but some dynamic problems may arise. During the cold rolling process, the strip is worked in several passes (up to over ten). In each pass, the work rolling speed changes because of the thickness reduction in the strip. Consequently, the rotational speed of rolls and back bearings increases up to five times. This leads to a wide range of frequency of dynamic

phenomena associated. In this case, continuous monitoring of dynamic behavior helps the operators in controlling the process and ensures a safe service.

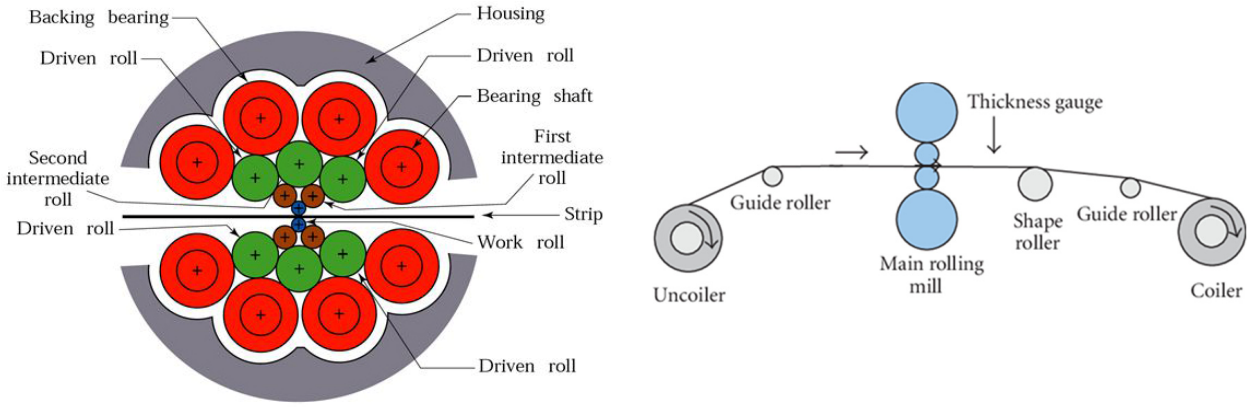

(**a**) (**b**)

Figure 1. (**a**) Layout of the Sendzimir cluster mill; (**b**) layout of the 4-high hot rolling mill.

In the cold rolling process, reaching the best surface finish possible is the main customer need. It requires that chatter marks and other defects are absent from the rolled product or at least reduced to a minimum size, negligible for the related application. To fulfill this requirement, the rolling mill must work regularly, with moderate mill cage vibration, small roughness of the working roll surface, and regular pressure distribution. Preferably, the temperature should not exceed 70 °C. Easy detection of any anomalous heating is therefore required, and this turns out into a need for a fast warning of operators provided by clear evidence of alert (sound, light, configuration change useful to trap the operators' attention).

In the hot rolling process, the geometric tolerances of the final product are different, but the health of working rolls in operation is a critical issue. As the temperature and its gradient across the cross-section of roll during system operation are higher, surfaces and structures suffer thermal stress, which usually leads to severe wear damage and thermomechanical fatigue [36]. Vibration monitoring is even important since it affects the product thickness [40]. Moreover, vibration may nucleate the damage to the mill equipment. It is worth noticing that the hot rolling mill usually includes few rolls, as in the 2-high and 4-high configurations (Figure 1b), being characterized by bigger and stiffer working and backup rolls, while in the cold rolling mill, the work roll is slender and smaller. Therefore, the two typical layouts differ quite a lot, and this is relevant for the access of the monitoring sensors.

2.3. The Mill Accessibility and Analysis of Monitoring Paths and Technologies

Some previous analyses based on the model-based system engineering [41] identified the fiber optic sensors [42] and piezoelectric microsensors [43] as the preferred choice for designing the monitoring system of the rolling mill. Piezoelectric sensors, associated with a telemetric unit, an energy storage system, and a microelectronic unit for the analysis and processing of data [29], need to be located in the proximity of monitored elements. This solution looks suitable for back bearings because of their size, while their application to work and support rolls is more difficult. They include some electronic circuits exposed to the risk of short-circuiting, especially in a harsh environment. The presence of flammable lubricant makes the effects of short circuits uncontrolled. The reliability of wireless communication even needs to be assessed [24,32]. Since the microelectronic units need to be very close to the monitored elements, in the cold rolling mill, interference, and noise, due to saddles of back bearings (see Figure 2, part 28) affect the communication.

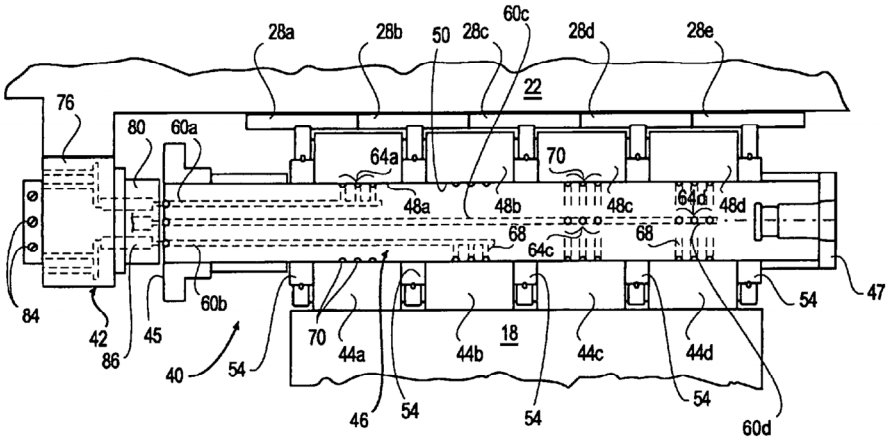

Figure 2. Back bearing assembly of a cluster mill [44].

Overcoming those limitations is possible by resorting to fiber optic sensors. The fiber Bragg gratings (FBG) sensors offer many advantages since they are intrinsically passive elements and can be installed even in hazardous environments. They are insensible to electromagnetic interference and provide a smooth operation, even at high temperatures. In addition, the interrogation instrumentation connected to FBG sensors can be installed even far from sensors, and thus the obstacles to the access of inner elements of the mill are less effective than in the case of wired MEMS. It is true that FBG is never autonomous in terms of power supply, and they need a main system emitting and receiving light, but the length of connection is less critical than in wired devices.

According to current industrial practice, in the rolling mill, the spin speed, lubrication condition, acoustic emission, load, and vibration amplitude of bearings are often monitored, as well as vibration and temperature [45]. Those measurements are seldom performed all simultaneously, i.e., a set of data allowing monitoring of the system in operation is collected during a duty cycle by measurements discretized in time. The location of the measuring device is usually quite far from the area of material processing, and some data can only indirectly monitor the machine condition, as in working rolls and bearings.

Frequency and vibration amplitude detected in the mill bearings reveal the presence of damages in either the inner or outer raceways and thus allow performing the "in-monitoring" [46]. Measuring the strip speed, in addition to its damages [47] or the motors' rotational speed [48], allows for identifying the mean speed of rolls, although the cluster layout is quite different between rolls. Due to their location, back bearings are suitable to measure the system dynamics, which allows for predicting some surface defects in the rolled strip ("out-monitoring"). Temperature monitoring may detect a severe anomaly within the system and helps in the prognosis of rolls undergoing thermomechanical fatigue [36]. Load measurement is beneficial in both the cold and hot rolling mills to control the pressure distribution on the rolled product.

To provide a synthesis, and according to the above-mentioned needs and practices, respectively, in the cluster mill, the monitoring activity can be performed at back bearings. Since they hold thin inner rings, poorly suitable for the installation of sensors along their radial direction, and external rings rotate, the FBG sensors can be installed just by resorting to their fixed pins. In contrast, in the hot rolling mill, the FBG sensors can be installed into the outer ring of either supporting or backup bearings when present. In this case, the inner ring is fixed and is constrained to the mill cage. For temperature monitoring of working rolls, sensors can be installed inside the roll. It is known that fiber optics sensors can be embedded in the roll geometry, in close proximity to the surface, and the interrogation module, together with additional modules required to perform the pre-analysis and dispatch of signal, can be installed at one end of the roll on their cross-section, just in front of access exploited by the operators [39].

Main monitoring activity will include the measurement of pressure applied by rolls on the rolled product, vibration amplitude of the mill cage, temperature of inner elements, and spin speed, at least of some rolls. Those measurements are performed every rolling pass at different speeds. The aim is to detect the mill dynamic behavior in operation at both the lower and higher frequency range. Particularly, the MCM will detect the chattering phenomenon, occurring at a higher frequency, usually appearing at some kHz, in cold rolling (1 to 10 approximately and depending on the mill layout and size).

Those MCM targets often motivate mounting some accelerometers on the mill cage to measure vibration and some load cells on working rolls. Nevertheless, an additional measurement at bearings should be welcome to prevent failures. The technology of capacitive MEMS sensors, already tested in this field [49], does not look effective because of the huge load applied (several MN at least) and of high temperature.

Exploiting the fiber optics technology for direct measurement of the mill cage vibration and for monitoring load, temperature, and damage in bearings seems promising. Fiber optics are never affected by problems related to electromagnetic compatibility, while, for instance, self-sensing piezoelectric sensors [50], which have been already proposed for monitoring the inner ring vibration in bearings, look poorly compatible with loading conditions because of their material brittleness. In contrast, fiber optics are free from ECM, thermal, and loading issues when suitably applied to monitored elements, as is herein described.

2.4. Proposed System: FBG Sensors Applied to Health Monitoring of Rolling Mill

The monitoring activity can be carried out starting from signals retrieved by the FBG sensors after a preliminary analysis performed by a unit installed in proximity of the rolling mill. External actions acting on the optic sensors, such as strain, temperature, and vibration, cause a variation in the Bragg wavelength [51,52]. The "Bragg gratings" allow setting up local, intrinsic, and absolute sensors to be operated even with multiplexed signals. The fiber core is treated to exhibit a periodic modulation of the material refractive index. The local sensors look like a sequence of mirrors, namely the Bragg gratings. Their refractive index is intentionally modified. They are distributed along the fiber and are variably spaced to each other, only partially reflecting the signal injected [53]. The diffractive phenomenon allows each grating to reflect a signal at a frequency related to spacing. This geometry allows the detection of any changes in temperature [54], strain, and pressure. The sensor plays the role of a dielectric mirror, able to reflect a specific frequency of light while transmitting all of the other ones.

If one analyzes separately several monitoring options, details allow for identifying some key issues of design. Particularly, measuring the displacement of signal peek in the dynamic response spectrum measured by the FBG sensor allows detecting the amplitude of the external agent and tracing its effect. The main parameter is the wavelength reflected by the Bragg grating, λ_B, which complies with the Bragg condition:

$$\lambda_B = 2n_{eff}\Lambda \tag{1}$$

where Λ is the grating pitch, being the distance between grating targets, and n_{eff} represents the effective refractive index of the given propagation mode. This is similar to the refractive one, but it is approximated with negligible error for the wave propagating inside transversely limited media as a function of the refractive index of the core and cladding of the optical fiber as in [51]:

$$n_{eff} = n_{cladding} + \left(1.1428 - \frac{0.996}{v}\right)^2 \Delta n \tag{2}$$

where $\Delta n = n_{core} - n_{cladding}$ and ν is a function of Δn and of the wavelength λ of light.

Several physical actions applied to the sensor, such as strain, temperature, and pressure, change the Bragg wavelength λ_B, and the measure of peak shift in the spectrum allows for calculating the corresponding change in the physical action. Particularly, if X is the generic physical signal, its influence upon the Bragg wavelength is:

$$\Delta\lambda_B = \frac{d\lambda_B}{dX}\Delta X = \lambda_B\left(\frac{1}{n_{eff}}\frac{dn_{eff}}{dX} + \alpha\right)\Delta X \quad (3)$$

where the first term within brackets represents the normalized sensitivity on the selected physical agent X (i.e., temperature, pressure, strain ...) of the effective refractive index, while α is a parameter related to the wavelength shift, expressed as a function of the physical signal X. A typical FBG optical sensor has a physical length of a few millimeters, a reflected bandwidth lower than 1 nm, and it might achieve the 100% reflection of the peak luminous intensity [52].

In strain measurement, the Bragg wavelength changes linearly [53], i.e., the proportionality factor denoted as strain sensibility coefficient, K_ε, is defined as:

$$\Delta\lambda_\varepsilon = K_\varepsilon\Delta\varepsilon \approx [0.78\lambda_B]\Delta\varepsilon \quad (4)$$

Since λ_B is approximately equal to 1550 nm, a typical value of K_ε is 1.2 nm·m/mm [54]. Experimental evidence demonstrated that response remains linear with strain, without hysteresis up to 400 °C.

The FBG sensors allow measuring vibration by detecting the frequency of dynamic excitation through a sort of firm of the working machine in operation, and the amplitude of dynamic response as the reflected signal exhibits a shift in frequency depending on the loading condition. Dynamic measuring needs employing a dynamic interrogator, being capable of sampling the signal typically at 1 kHz and even higher frequency, and thus the system cost increases. The longitudinal strain of fibers is exploited for this measurement to assure a suitable sensitivity of the sensor to signal. To make more effective the monitoring system, in the literature is known the use of vibration sensors, based on a small flexible structure equipped with fiber optics, to be connected to the monitored structure, which exploits the forced vibration of a small cantilever (Figure 3) [55].

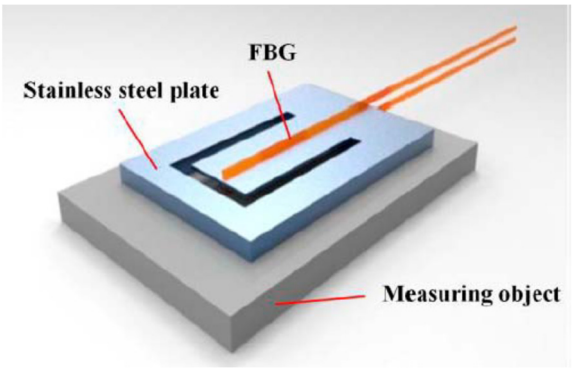

Figure 3. FBG-based finite vibration sensor used to emphasize the dynamic excitation of monitored structure [55].

A contactless measurement is even performed, by focusing the sensor on a thin vibrating element, equipped with a small permanent magnet, whose vibration is excited by the rotating shaft, without direct contact. More in general, a displacement sensor is even based on a couple of fibers, one transmitting and one receiving light, respectively, which focus on a target in motion to detect its relative position with respect to the sensor location.

The FBG sensors are even used in monitoring pressure. Measuring pressure lower than 1 bar is difficult. In contrast, when pressure changes quite fast, these sensors allow monitoring even a sudden evolution of operating conditions. Pressure is measured through the Poisson's effect on the fiber's material. If the fiber is assumed to be sufficiently long to avoid any additional local effect of ends, strain is related to pressure applied on the lateral surface as follows:

$$\begin{aligned} \varepsilon &= \tfrac{\Delta P}{E}(1-2v) \\ \Delta\lambda_B &= K_P\Delta P \end{aligned} \quad (5)$$

where ε is the axial strain of fiber, ΔP is the gradient of pressure in time, E is the Young modulus of the fiber's material (typically $E \approx 72$ GPa, in silicon composites, or $E < 30$ GPa in case of polymeric coating with relevant thickness) and v is the Poisson's coefficient. The sensitivity on pressure change is given by $\Delta\lambda_B$, and in standard fibers, can be quite low, although, in the literature, some examples of polymeric coatings can be found leading to a coefficient K_P of up to 34 nm/MPa.

It is known that by introducing the temperature sensibility coefficient, K_T, Equation (3) becomes:

$$\Delta\lambda_T = K_T \Delta T \tag{6}$$

being linear only within a limited range of temperature values (typically below 100 °C). When a greater temperature range is expected, it is preferred to express the temperature sensitivity coefficient as a function of the thermal expansion coefficient of fiber, α_0, and of thermo-optic coefficient, β_0, as $K_T = \lambda_B\ (\alpha_0 + \beta_0)$, by resorting to a second-order formula for β_0, which allows describing its sensitivity on temperature [56]. It is worth noticing that temperature variation of n_{eff} deeply depends on the characteristics of the fiber, and even a small difference in material and production technique can strongly affect those coefficients, as in [57], where another application of FBG sensors is applied to steelmaking, but limitedly to the copper plate for melting and cooling.

Equation (3) clearly states that the signal of a single FBG sensor does not distinguish the contribution induced by strain and by temperature, respectively, to the measured value. In the case of vibration detection, the temperature variation normally occurs at a frequency that is largely lower than the vibration frequency. In static or quasi-static analysis, this becomes a problem since the two sources of strain are coupled. Therefore, it is required to resort to a measuring system consisting of at least two sensors:

$$\begin{pmatrix} \Delta\lambda_1 \\ \Delta\lambda_2 \end{pmatrix} = \begin{bmatrix} K_{1\varepsilon} & K_{1T} \\ K_{2\varepsilon} & K_{2T} \end{bmatrix} \begin{pmatrix} \varepsilon \\ T \end{pmatrix} = [K] \begin{pmatrix} \varepsilon \\ T \end{pmatrix} \tag{7}$$

where $K_{i\varepsilon}$ and K_{iT} are the strain and temperature sensitivity coefficients of the i-th sensor, respectively. Excluding the special case in which every sensor is sensible only to one of the two above-mentioned perturbations, two configurations are foreseen. When the measurement of one sensor, at least, is affected only by one of the two physical perturbations, i.e., one element of matrix K is null, that sensor becomes the reference to uncouple the two signals composing the system response. When the sensitivities of the two sensors are just moderately different, and the determinant of matrix K is defined, i.e., not null, a numerical solution to the above Equation (7) is found. It is worth noticing that using FBG sensors, whose sensitivities have both non-null values, implies resorting to the second case here described above. Producing FBG sensors with different sensitivity is possible, for instance, by exploiting fibers with different diameters spliced together. A technical difficulty arises in splicing together fibers whose diameter is different. Moreover, even inscribing the FBG in the fibers' core is difficult. This type of configuration cannot be applied in embedded fiber because both sensors would result in being bound to the structure and undergoing the same strain, and thus matrix K would be singular. Those are the main limitations of the proposed approach, but a technical solution is available.

Resorting to two FBG sensors, made with different Bragg wavelength λ_B allows handling those problems. According to Equation (3), FBG sensors exhibiting different central wavelengths also have different strain and temperature sensitivity coefficients. Therefore, inscribing both sensors on the same fiber and using an interrogator capable of detecting a multitude of wavelengths allow solving Equation (7), provided that all parameters of sensors are known. To avoid the case of badly conditioned matrix K, a difference of at least 10% in Bragg wavelength between the two sensors is required [58]. Some suitable values of λ_B have already been tested in some commercial FBG sensors and result in 850 and 1300 nm, or 1300 and 1550 nm, respectively. Therefore, the configuration here described above looks suitable for a coupled measurement without a real problem of the distinction between monitored physical entities. Moreover, the overall size of

sensors corresponds to the dimensions of fibers. This allows for embedding sensors in the mechanical system and sometimes even in the material of components. They look minimally invasive, and they allow avoiding a significant structural weakening effect. Finally, the wavelength division multiplexing (WDM) technique allows exploiting several sensors [59], composing a network applied to the monitored system, and thus the cost and complexity of the monitoring system are significantly reduced.

3. Results

3.1. Proposed Architecture and Operation of Monitoring System

The application of the above-mentioned monitoring system differs in the case of cold and hot rolling mills, respectively. The typical layout to be considered in cold rolling is the cluster mill with multiple rolls (up to 20, usually) (Figure 4). In this case, monitoring the pressure applied by each bearing of the backup roll on the cage pin is significant to detect any anomalous loading condition, dynamic response, temperature change, and even local damage evidence.

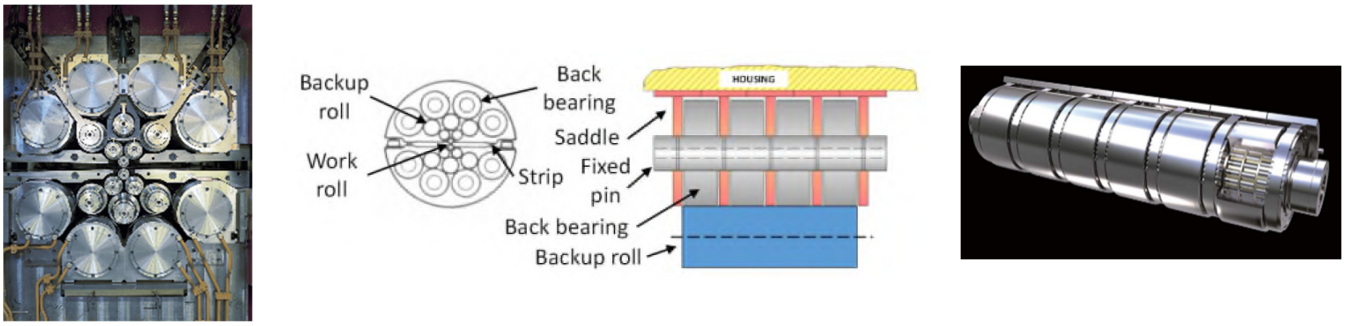

(**a**) (**b**) (**c**)

Figure 4. Layout of cluster mill with inner fixed pin: picture (**a**) [60], sketch (**b**), and rendering (**c**) [61].

The fiber optic sensor can be deployed along the fixed pin (Figure 5) by eventually exploiting the lubricant feed channels 60a, 60b, and 60c in Figure 2, or similar since the massive constitution of the pin allows the creation of some additional channels, even smaller to embed the fiber optics sensors. The external head 42 (Figure 2) allows locating the required connections to the interrogator and demodulator devices, as connectors 84 do for the lubrication system. Exploiting separated channels, being eventually filled by liquid, reduce the risk of early deterioration of fiber coatings, particularly if lubricant feed channels were preliminarily selected to guest fiber optics. Measurements are performed at dedicated locations as 64a and 70 or similar. One sensor can reach the inner ring of the backup bearing to detect the local pressure along an arc of the circumferential deployment of fiber optic installed inside the pin, just below the inner ring, as it was even performed in the case of bearing housing in the work of [62]. Measurement of local temperature can be performed at a dedicated cavity produced on the pin surface in correspondence to the inner ring.

Similarly, a double set of fiber optic sensors can be applied to rolls of the hot rolling mill by resorting to the structure of the vertical positioning system, which directly controls the outer ring of main bearings (Figure 6). In the case of roller bearings, pressure and temperature monitored are those closest to the main body of rolls. In addition, optical measurements assure monitoring of the strip temperature, while some load cells help in controlling the load applied to the work roll. Eventually, the local measurements can be applied to several points to have at least some discretized access to pressure and temperature distributions with the bearing. A similar arrangement could even be conceived for lubricated bearings and aims at detecting the effect of load on the elastic deformation of rings to improve the prediction by modeling of the gap inside the bearing layout.

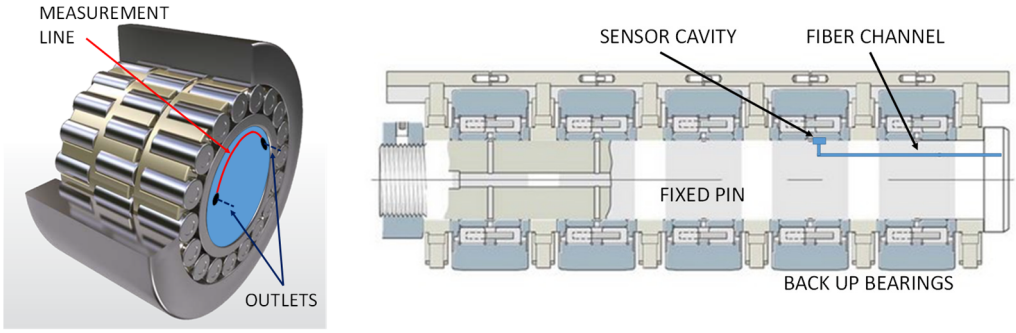

Figure 5. Example of location of sensors for pressure (**a**) and temperature (**b**) measurement in the backup bearing of a cluster cold rolling mill drawn upon rendering of bearing [61] and assembly [63].

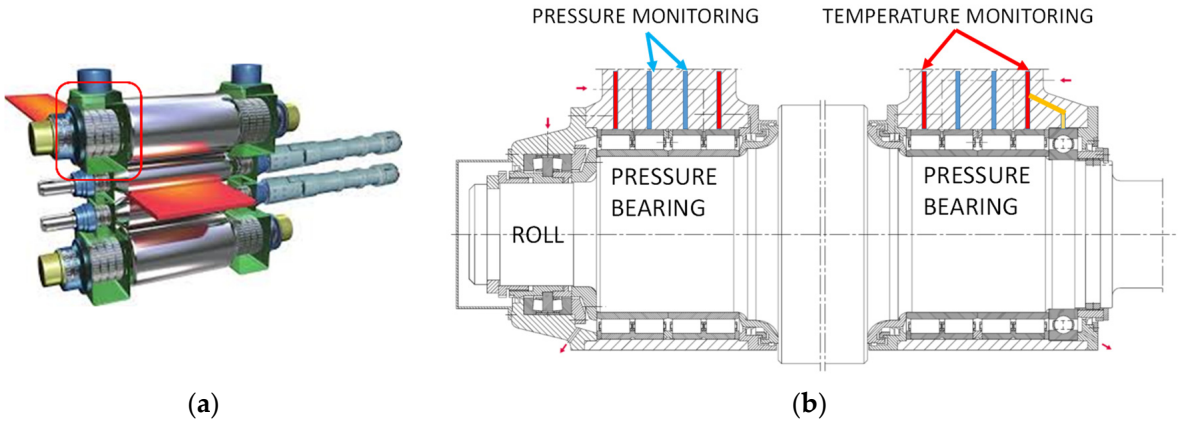

Figure 6. Example of location of sensors for pressure and temperature measurement upon back bearings of a hot rolling mill drawn upon rendering of bearing (**a**) and assembly (**b**).

3.2. Experimental Set-up for Thermal Monitoring

After selecting the smart bearing technology and the most accessible path within the mill cage, a preliminary design of the monitoring system is performed. A preliminary technological assessment on a test rig helps in checking the suitability of the proposed approach. Validation on a real plant is then required, despite the cost and some practical issues related to the implementation of a full-scale system. Practically speaking, the main issues of this design include the first characterization of FBG sensors when monitoring pressure and load applied to bearings, as well as vibration, and then when measuring temperature. In the latter case, a current discussion in the literature is how the sensor must be located upon the monitored structure, resorting to a dedicated cavity. Particularly, shaping and filling of the cavity are additional design issues, as the literature proposes some solutions of operation in either oil or air. Moreover, the design of FBG sensors for the rolling mill has to take into account several targets, such as failure detection, predictive maintenance of elements, and prevention of combustion, with associated automatic alarming action.

Considering the above-mentioned tasks, the literature already demonstrated the possibility of equipping bearings with FBG sensors for measuring the pressure applied to its raceways in operation. Particularly, this application is not so far from the case analyzed in [62], providing a complete demonstration of operation, despite the different sizes and applications considered. Those demonstrations fit the requirements of the rolling mill. Therefore, a further discussion about that task seems poorly attractive in this paper. Many approaches have been inherently developed based on soft computing techniques [64], multiwavelet denoising [65], and isolation of bearings' signals in drivers [66].

In contrast, the measurement of temperature through the FBG sensors looks intrinsically a current topic of the literature when applied to steelmaking [67]. Temperature detection is required to uncouple mechanical from thermal excitation, respectively, as has been previously discussed. In both the hot and cold rolling mills, the detection of a temperature higher than 70 °C at the two locations selected, i.e., close to the inner ring in the cluster mill and to the outer ring in the hot rolling mill, may reveal an incipient condition of failure, and surely an undesired working condition for lubricant. It is sufficient to need warning operators while a temperature above 100 °C activates an alarm.

Moreover, the detection of temperature in warning and alarm conditions, respectively, must be fast, evident and intuitive for operators, as well as safe for the overall system. Those motivations lead to exploiting water to fill the cavity where the FBG sensor is recovered, more than lubricant. A sacrificial layer can even be used to cover the inner surface of the cavity, being made with a material whose melting point is close to 70 °C. It could emphasize the alarm signal by coloring the water flowing back from that cavity, where the FBG sensors are monitoring temperature. Therefore, a key issue for the technological assessment of the monitoring system looks at the design of the cavity and the selection of material surrounding the fiber.

The FBG sensors assure appreciable linearity of their response in operation. They are operated in multiplexing mode by inscribing several sensors on the same fiber. A precise calibration allows exploiting all those benefits. Nevertheless, an open question, in the case of the cavity embedded in the inner elements of the mill cage, concerns the effectiveness of measurement. Some preliminary experiments have been performed upon a set of FBG sensors inscribed on a single-mode fiber, with an outer diameter of cladding equal to 125, core diameter of 9 μm, and total length of 4 mm. Preliminary characterization of FBG sensors has been completed by identifying their thermal sensitivity coefficient through a direct comparison with a thermo-resistor PT-100. The goal of this calibration is the identification of $\Delta\lambda_B$ for a given change of temperature, and thus the determination of K_T as the slope coefficient of the characteristic function $\Delta\lambda_B = \Delta\lambda_B(T)$.

In this test rig, a Peltier cell, driven by the controller TEC ("Thermo-Electric Controller") TEC-1091 (Meerstetter Engineering GmbH, Rubigen, Switzerland), imposes the temperature changes in measurement activity. The controller TEC-1091 has an input voltage of 5 to 24 V (DC), output voltage of 0 to ±21 V, and output current of 0 to ±4 A. The TEC controller regulates the current feeding the Peltier cell through a PID control, whose feedback acts on the error between the value of temperature defined by the user and that measured by the PT-100. The thermos-resistor RSPro PT-100 (Platinum) operates within the range of −50 to +250 °C by resorting to a "four wires" configuration, resistance at a melting point is 100 Ω, sizes are 2 mm (width) and 10 mm (length), while tolerance class is A.

The FBG sensors have been connected to the SmartScan Interrogator (Smart Fibers Ltd., Bracknell, UK), which operates in dynamic mode. It analyzes up to 4 fibers and a maximum of 16 FBG sensors through the WDM method ("wavelength division multiplexing method"). The experimental campaign exploited a single fiber with one sensor during each test. The main properties of sensor FemtoFiberTech (FemtoFiberTec GmbH, Goslar, Germany), based on fiber SM1250BI, are the core diameter of 9.8 μm, cladding diameter of 125 μm, coating in polyimide, central wavelength of 1565.07 nm, sensor length of 3.2 mm, reflectivity of 71.4%, bandwidth at 3 dB 0.47 nm, and signal-to-noise ratio of 25.6 dB. The communication between interrogator and PC host is assured through the Ethernet and the software SmartSoft SSI v3.2 (Smart Fibers Ltd., Bracknell, UK).

The sampling frequency of 2.5 kHz allows reaching a compromise condition between the need of retrieving as many data as possible and the limitation of the frequency range induced by a high number of samples. That frequency allows for detecting signals within the range of 40 nm. The interrogator is aimed at detecting the amplitude of the reflected component of the signal within the frequency range defined. Wavelength stability is assured within ±5 pm, within the temperature range −10 to +80 °C, optical connectors FC/APC with a diameter of 2.5 mm of bushing.

The Peltier cell used in testing is TEC1-12706 with a maximum current of 3 A, maximum voltage of 8.6 V, maximum power of 20 W, maximum difference in temperature of 66 °C, sizes 23 × 23 × 3.6 mm, and weight of 26 g.

3.3. Effect of the Fixing Typology on the Temperature Response of the Sensor

Some tests have been carried out to investigate several design issues, looking critical in the case of the rolling mill layout. The first one focuses on the constraints applied to fiber optic sensors. The FBG sensor has been fixed in direct contact with the warm surface of the Peltier cell, by means of a bolted device, with four bolts and a sheet of metal and never loaded above 1 Nm (tightening torque). This configuration might replicate the geometry of the hot rolling mill depicted in Figure 6, for instance (Figure 7a).

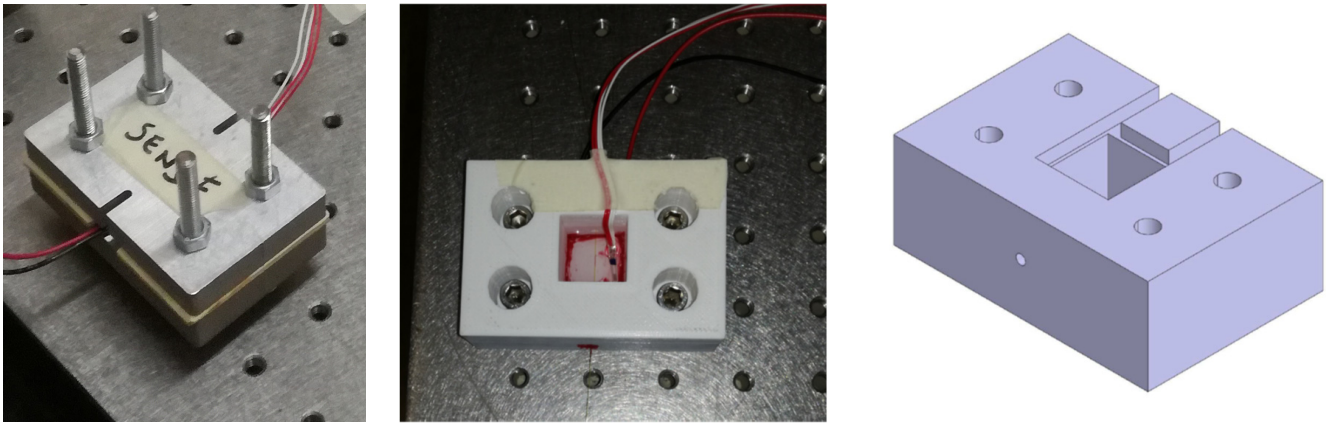

(**a**) (**b**) (**c**)

Figure 7. Bolted system holding the FBG sensor (**a**), cavity filled with water (**b**), 3D-printed support with measurement room filled with water, and hole for FBG sensor access (**c**).

Direct contact under pressure reveals several drawbacks. During tests, some samples of fiber were broken because of pressure imposed by bolts on their imperfect location inside the room created in correspondence of surfaces. Despite the possibility of uncoupling the two signals of temperature and pressure, respectively, as it was mentioned above, the strong constraint applied to fiber along the lateral direction, inhibiting the Poisson effect from working properly under temperature changes, introduced an error of up 100% on the determination of K_T, for a given increment of bolt loading of 20%. Particularly, on a set of 10 samples, tests demonstrated that for ΔT = 20 °C, $\Delta\lambda_B$ varies from 0.24 nm (at 0.6 Nm) to 0.35 nm (at 0.8 Nm), and then 0.49 nm (at 1 Nm). Moreover, comparing the temperature imposed by the cell and that measured by the FBG sensor, being in simultaneous contact with the supporting plate and the surface of the Peltier cell, it was realized that a significant time delay occurs to find the two values of temperatures superposed (up to 550 s). The FBG sensor is simultaneously in contact with the supporting plate and the hot surface of the Peltier cell, and thus a sort of average value of temperature is measured until that thermal equilibrium is established. This might reduce the promptness of the measuring system if some transient effects are monitored.

That evidence confirms the need for a cavity to surround the fiber to have a faster thermal equilibrium assessment. This solution was already tested in [57], with a cavity of 10 × 10 mm and a depth of 3 mm, creating a bubble of air around the fiber. In that case, the monitored process is aluminum solidification in a sand mold. A stainless steel tube encased the optical fiber to allow it to survive both mechanical and thermal conditions, as it demonstrated reaching 700 °C without failures. The efficiency of air bubbles in the present case has been tested, with very poor results. Nevertheless, filling the cavity with demineralized water allowed reaching better results (Figure 7b). To perform this experiment, a specific device has been built up in thermoplastic resin and through 3D

printing. The FBG sensor can cross a central room filled with liquid, being water in this test, in contact with the hot surface to be monitored through some holes produced on the lateral surfaces. A final set of tests has been performed to characterize the FBG sensor in thermal measurement, located in the new holding system depicted in Figure 7c.

3.4. Thermal Response and Sensibility Tests

Tests investigated the range of temperatures of 30 to 70 °C, considering that the material of the 3D-printed device exhibits a melting point at 75 °C. This property, in real operation, might help in visualizing the effect of temperature since the melt thermoplastic resin adds white color to water and, thus, the operator can receive an additional visual warning of the risk of excessive heating. The use of water might even help in perceiving the achievement of 100 °C as soon as it starts boiling. The cooling water jets applied to rolls, for instance, assures the availability of water at room temperature.

The temperature has been increased by a rate of 0.02 °C/s. Ten tests allowed extracting the main properties of the FBG sensor as follows:

$$\{\lambda_i\} = K_T\{T_i\} + a \tag{8}$$

i.e., a linear regression based on the minimum squares method allowed finding the relation between measurement and temperature, considering parameter '*a*' the wavelength at 0 °C.

To validate the numerical approach, the determination coefficient R^2 is defined as:

$$R^2 = \frac{\sum_{i=1}^{n}\left(\widetilde{\lambda}_i - \overline{\lambda}\right)^2}{\sum_{i=1}^{n}\left(\lambda_i - \overline{\lambda}\right)^2} \tag{9}$$

has been calculated by comparing measured values λ_i, their average value $\overline{\lambda}$, and values $\widetilde{\lambda}_i$ obtained by the linear regression.

The uncertainties related to experimental parameters required resorting to the Monte Carlo method [68,69] to check the reliability of numerical values extracted by the linear regression. Both the temperature and wavelength signals are subject to measurement errors due to the sensitivity of the measuring instruments. In particular, the uncertainty of the measuring equipment was used to define the standard deviation (s) of the temperature signal, $s(T_i)$ = 0.01 °C, and wavelength signal, $s(\lambda_i) = 8 \times 10^{-4}$ nm. In order to evaluate the standard deviation of the linear regression coefficients, $s(K_T)$ and $s(a)$, using a Monte Carlo simulation, 5000 runs were carried out for each test, randomly varying each of the measured values within the uncertainty interval (represented by plus or minus one standard deviation from the experimentally measured value), according to a uniform distribution. The five thousand linear correlation values thus obtained were used to evaluate the standard deviation of both linear regression coefficients, obtaining $s(K_T) = 1 \times 10^{-5}$ nm/°C and $s(a) = 1 \times 10^{-3}$ nm. Therefore, for each test, the temperature sensibility coefficient K_T can be considered correct up to the fourth decimal place, while the parameter 'a' can be considered certain up to the second.

Tests lead to evaluate main parameters varying within a narrow range of values, since K_T = 0.01207 to 0.01272 (nm/°C) with a = 1564.913 to 1564.960 (nm), R^2 = 0.9979 to 0.9997, λ_0 = 1565.292 to 1565.326 (nm). The average value of K_T is 0.01232 nm/°C with variance $\sigma^2 = 3.661 \times 10^{-8}$ (pm/°C)^2. This result demonstrates the suitable reliability of that identification. It can be noticed that the interrogator can measure changes in temperature corresponding to $\Delta\lambda_{min}$ = 0.0008 nm. Therefore, the minimum change of temperature to be detected is $\Delta T_{min} = 0.0008/K_T$ = 0.065 °C, i.e., 100 times the precision of the controller TEC equipped with thermocouple PT-100. The correspondence between the regression function and experimental results has been checked as well as the linearity of the dynamic behavior of the FBG sensor (Figure 8).

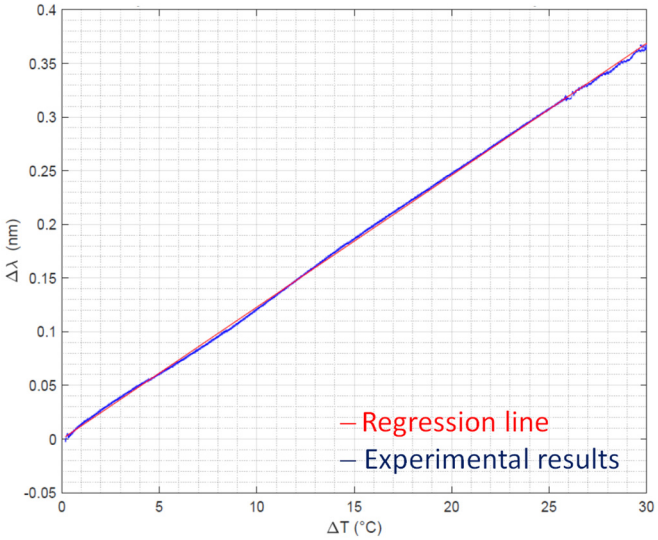

Figure 8. Characterization of the FBG sensor and comparison between mathematical approximation and experimental results.

4. Discussion

The health monitoring of the rolling mill includes a careful measurement of vibration and temperature in service, despite the difficulty of access to the mill cage and to bearings, in particular. Therefore, in a preliminary step, this investigation analyzed the layout of the rolling mill, and some possibilities have been found:

- In the cold rolling mill, the fixed pins of backup bearings are suitable to host the fiber optics sensors to monitor the temperature of the inner rings of bearings;
- In the hot rolling mill, the system constraining the outer rings of bearings allows access to the fiber optics sensors.

A second step has been focusing on the sensors' technology:

- The FBG sensors look suitable for this application, although the assembling system may be critical for measurement. Particularly, the FBG sensor suffers the effect of pressure and/or of structural deformation.

A third level of details includes some recommendations for the assembly:

- Creating a cavity where the sensor measures temperature allows uncoupling of the effect of pressure and of temperature, respectively;
- Thermal measurement may benefit from filling the cavity with either a liquid or gas. In principle, this material might consist of air bubbles, but the performance in terms of promptness and uniformity of temperature is poorly evident. Demineralized water allows surrounding the fiber and transferring heat quite fast and uniformly, although the use of water must be verified for all industrial layouts currently used.

Materials selection might consider some properties of the monitoring system as detectability of temperature:

- If the system must never be operated above 70 °C, a sacrificial layer made of thermoplastic resin, whose melting point is around 75 °C, deposed on the surface of the cavity, might help in warning the operators when the maximum temperature is reached. In principle, above 100 °C boiling could add an intuitive alarm, provided that no other problems are foreseen.

The operation of the FBG sensors looks feasible and practical after a preliminary calibration of the monitoring system. As it was demonstrated in the previous section, by experiment, reliable identification of the main parameters useful for the measurement activity is assured, despite the number of steps that require an accurate implementation. The sensitivity of the FBG sensor looks even better than in other technologies.

The harsh environment significantly affects the monitoring system behavior, in general, but the FBG sensors allow reaching a high temperature, are remotely controlled, look suitable to access the inner parts of the mill cage, and do not suffer the interaction with electric and magnetic fields.

The cost of FBG sensors is never negligible because of the number of elements composing the monitoring system. Nevertheless, the technological benefits of fiber optics and the availability of a reliable monitoring system combined with the overall cost of the mill may allow considering this solution feasible for a real smart manufacturing implementation. It is true that only a systematic approach, such as the model-based systems engineering used in the case of aircrafts, for instance [70], will allow the development of the whole monitoring system, and the heterogeneous simulation tools [71] nowadays available will allow for integrating the network of distributed sensors within the mill cage elements.

5. Conclusions

The steelmaking process is surely expensive in terms of power consumption, energy dissipation, and pollution and requires a drastic reduction in waste, energy, and material. It requires a very high safety assurance for the operators against the risk of injuries.

In this study, a contribution to smart manufacturing based on process monitoring has been proposed. The literature often focuses on monitoring either the rolled product by some contactless measurements or on the system control through some actuators (motors, hydraulic actuators, etc.). Bearings are seldom the target of monitoring if they resort to mechanical components based on either rolling elements or fluid film.

The first matter of discussion is the location of distributed sensors to be applied to the mill elements to detect damage, vibration, and heating phenomena. Considering the layout of hot and cold rolling mills mostly used, some solutions have been analyzed to overcome several difficulties in accessing the inner parts of the mill cage. The FBG sensors look highly compliant with the limitations of the mill layout. Particularly, they allow measuring the temperature of structural components as bearings very precisely and uncoupling some other effects such as those induced by electric and magnetic fields. Nevertheless, some practical issues have been circumstantiated, such as the need for a cavity for locating the fiber optic close to the monitored surface to avoid direct pressure on thermal sensors. Filling the cavity with a liquid helps in making uniform and easily detectable temperature. A preliminary experimental demonstration confirmed the suitable performance of the FBG sensors in such an embedded environment.

The next step requires a direct implementation of a working rolling mill to check all the technological issues related, i.e., the large size of the mill system, the harsh environmental conditions, and the superposition of physical noise and interferences in service.

Author Contributions: Conceptualization, E.B., C.D. and L.G.; methodology, E.B., C.D. and L.G.; investigation, L.G.; writing—original draft preparation, E.B. and L.G.; writing—review and editing, E.B. and C.D.; supervision, E.B. and C.D. All authors have read and agreed to the published version of the manuscript.

Funding: This research received no specific external funding.

Conflicts of Interest: The authors declare no conflict of interest.

References

1. Rentz, O.; Jochum, R.; Schultmann, F. *Report on Best Available Techniques (BAT) in the German Ferrous Metals Processing Industry*; Deutsch-Französisches Institut für Umweltforschung (DFIU): Karlsruhe, Germany, 1999; pp. 1–149.
2. Brusa, E.; Lemma, L. Numerical and Experimental Analysis of the Dynamic Effects in Compact Cluster Mills for Cold Rolling. *J. Mater. Processing Technol.* **2009**, *209*, 2436–2445. [CrossRef]
3. Flick, A.; Fliegel, G. Trends in the Steel Industry: Innovative Solutions to Drive Sustainability. *Trans. Indian Inst. Met.* **2013**, *66*, 535–541. [CrossRef]
4. Verma, N.K.; Salour, A. *Intelligent Condition Based Monitoring: For Turbines, Compressors, and Other Rotating Machines*; Studies in Systems, Decision and Control; Springer: Singapore, 2020; Volume 256, ISBN 9789811505119.

5. Brunton, S.L.; Kutz, J.N. *Data-Driven Science and Engineering: Machine Learning, Dynamical Systems, and Control*, 1st ed.; Cambridge University Press: Cambridge, UK, 2019; ISBN 978-1-108-38069-0.
6. Brusa, E. Development of a Sentry Smart Bearing as a Node for Connectivity and Monitoring of Steelmaking System. In Proceedings of the 2017 IEEE International Systems Engineering Symposium (ISSE), Vienna, Austria, 11–13 October 2017; pp. 1–8.
7. Brusa, E.; Bruzzone, F.; Delprete, C.; Di Maggio, L.G.; Rosso, C. Health Indicators Construction for Damage Level Assessment in Bearing Diagnostics: A Proposal of an Energetic Approach Based on Envelope Analysis. *Appl. Sci.* **2020**, *10*, 8131. [CrossRef]
8. Galar, D.; Kumar, U. SMART Bearings: From Sensing to Actuation. In Proceedings of the 12th IMEKO TC10 Workshop on Technical Diagnostics, Florence, Italy, 6–7 June 2013.
9. Shao, Y.; Ge, L.; Fang, J. Fault Diagnosis System Based on Smart Bearing. In Proceedings of the 2008 International Conference on Control, Automation and Systems, Seoul, Korea, 14–17 October 2008; pp. 1084–1089.
10. Mohanty, A.R. *Machinery Condition Monitoring: Principles and Practices*; CRC Press: Boca Raton, FL, USA, 2017; ISBN 978-1-4665-9305-3.
11. Randall, R.B. *Vibration-Based Condition Monitoring: Industrial, Aerospace and Automotive Applications*; John Wiley & Sons, Ltd.: Chichester, UK, 2011; ISBN 978-0-470-97766-8.
12. Elangovan, U. *Smart Automation to Smart Manufacturing: Industrial Internet of Things*; Momentum Press: Singapore, 2019; ISBN 1-949449-27-0.
13. Nirwan, N.W.; Ramani, H.B. Condition monitoring and fault detection in roller bearing used in rolling mill by acoustic emission and vibration analysis. *Mater. Today Proc.* **2021**, *51*, 344–354. [CrossRef]
14. Cusano, A.; Cutolo, A.; Albert, J. *Fiber Bragg Grating Sensors: Recent Advancements, Industrial Applications and Market Exploitation*; Bentham Science: Sharjah, United Arab Emirates, 2011.
15. Brusa, E.; Morsut, S. Design and Structural Optimization of the Electric Arc Furnace Through a Mechatronic-Integrated Modeling Activity. *IEEE/ASME Trans. Mechatron.* **2015**, *20*, 1099–1107. [CrossRef]
16. Lees, A.W. Smart Machines with Flexible Rotors. *Mech. Syst. Signal Processing* **2011**, *25*, 373–382. [CrossRef]
17. Genta, G. *Dynamics of Rotating Systems*; Mechanical Engineering Series; Springer: New York, NY, USA, 2005; ISBN 978-0-387-20936-4.
18. Genta, G.; Delprete, C.; Brusa, E. Some Considerations on the Basic Assumptions in Rotordynamics. *J. Sound Vib.* **1999**, *227*, 611–645. [CrossRef]
19. Brusa, E. Design of a Kinematic Vibration Energy Harvester for a Smart Bearing with Piezoelectric/Magnetic Coupling. *Mech. Adv. Mater. Struct.* **2020**, *27*, 1322–1330. [CrossRef]
20. Miśkiewicz, R.; Wolniak, R. Practical Application of the Industry 4.0 Concept in a Steel Company. *Sustainability* **2020**, *12*, 5776. [CrossRef]
21. Neef, C.; Hirzel, S.; Arens, M. *Industry 4.0 in the European Iron and Steel Industry: Towards an Overview of Implementations and Perspectives*; Fraunhofer Institute for Systems and Innovation Research (ISI): Karlsruhe, Germany, 2018; pp. 1–32.
22. Brusa, E. Digital Twin: Towards the Integration Between System Design and RAMS Assessment Through the Model-Based Systems Engineering. *IEEE Syst. J.* **2020**, *15*, 3549–3560. [CrossRef]
23. Holm-Hansen, B.T.; Gao, R.X. Vibration Analysis of a Sensor-Integrated Ball Bearing. *J. Vib. Acoust* **2000**, *122*, 384–392. [CrossRef]
24. Kovacs, A.; Peroulis, D.; Sadeghi, F. Early-Warning Wireless Telemeter for Harsh-Environment Bearings. In Proceedings of the 2007 IEEE Sensors, Atlanta, GA, USA, 28–31 October 2007; pp. 946–949.
25. Draney, R.K. High Temperature Sensor for Bearing Health Monitoring. In Proceedings of the 2008 IEEE Aerospace Conference, Big Sky, MT, USA, 1–8 March 2008; pp. 1–7.
26. Samson, D.; Kluge, M.; Becker, T.; Schmid, U. Wireless Sensor Node Powered by Aircraft Specific Thermoelectric Energy Harvesting. *Sens. Actuators A Phys.* **2011**, *172*, 240–244. [CrossRef]
27. Wang, W.; Jianu, O.A. A Smart Sensing Unit for Vibration Measurement and Monitoring. *IEEE/ASME Trans. Mechatron.* **2010**, *15*, 70–78. [CrossRef]
28. Winkelmann, C.; Woitschach, O.; Meyer, E.; Lang, W. Development of a Strain Sensor for Rolling Contact Loads. In Proceedings of the 2011 16th International Solid-State Sensors, Actuators and Microsystems Conference, Beijing, China, 5–9 June 2011; pp. 1080–1083.
29. Bashir, I.; Wang, L.; Harvey, T.; Zaghari, B.; Weddell, A.; White, N. Integrated Smart Bearings for next Generation Aero-Engines Part 1: Development of a Sensor Suite for Automatic Bearing Health Monitoring. In Proceedings of the 1st World Congress on Condition Monitoring, ILEC Conference Centre, London, UK, 13–16 June 2017.
30. Choi, D.; Sung, T.; Kwon, J.-Y. A Self-Powered Smart Roller-Bearing Based on a Triboelectric Nanogenerator for Measurement of Rotation Movement. *Adv. Mater. Technol.* **2018**, *3*, 1800219. [CrossRef]
31. Zhang, Y.; Cao, J. Development of Self-Powered Smart Bearing for Health Condition Monitoring. In Proceedings of the 2018 IEEE/ASME International Conference on Advanced Intelligent Mechatronics (AIM), Auckland, New Zealand, 9–12 July 2018; pp. 786–791.
32. Zaghari, B.; Weddell, A.S.; Esmaeili, K.; Bashir, I.; Harvey, T.J.; White, N.M.; Mirring, P.; Wang, L. High-Temperature Self-Powered Sensing System for a Smart Bearing in an Aircraft Jet Engine. *IEEE Trans. Instrum. Meas.* **2020**, *69*, 6165–6174. [CrossRef]
33. Cavaliere, P. *Clean Ironmaking and Steelmaking Processes: Efficient Technologies for Greenhouse Emissions Abatement*; Springer: Cham, Switzerland, 2019; ISBN 978-3-030-21208-7.
34. Lenard, J.G. *Primer on Flat Rolling*, 2nd ed.; Elsevier: Waltham, MA, USA, 2014; ISBN 978-0-08-099418-5.

35. Chang, D.-F. Thermal Stresses in Work Rolls during the Rolling of Metal Strip. *J. Mater. Processing Technol.* **1999**, *94*, 45–51. [CrossRef]
36. Benasciutti, D.; Brusa, E.; Bazzaro, G. Finite Elements Prediction of Thermal Stresses in Work Roll of Hot Rolling Mills. *Procedia Eng.* **2010**, *2*, 707–716. [CrossRef]
37. Chiesa, S. *Affidabilità, Sicurezza e Manutenzione nel Progetto dei Sistemi*; CLUT: Torino, Italy, 2008; ISBN 978-88-7992-264-7.
38. Sendzimir, M.G. The Sendzimir Cold Strip Mill. *JOM* **1956**, *8*, 1154–1158. [CrossRef]
39. Brusa, E.; Lemma, L. A Multi-level Approach for the Mechanical Design of Cluster Mills for Cold Rolling of Thin Steel Products. In Proceedings of the 8th Biennal ASME Conference on Engineering Systems Design and Analysis, ESDA, Turin, Italy, 4–7 July 2006; pp. 1–11, ISBN 0-7918-3779-3.
40. Xiao, B.; Yan, X. Research on Vertical Vibration of Hot Rolling Mill under Screw-down-Strip Combined Excitation. *J. Vibroengineering* **2019**, *21*, 2050–2063. [CrossRef]
41. Brusa, E.; Calà, A.; Ferretto, D. *Systems Engineering and Its Application to Industrial Product Development*; Studies in Systems, Decision and Control; Springer International Publishing: Berlin/Heidelberg, Germany, 2018; ISBN 978-3-319-71836-1.
42. Brusa, E.; Della Vedova, M.; Giorio, L.; Maggiore, P. Thermal condition monitoring of large smart bearing through fiber optics sensors. *Mech. Adv. Mater. Struct.* **2021**, *28*, 1187–1193. [CrossRef]
43. Ng, T.-H.; Liao, W.-H. Feasibility Study of a Self-Powered Piezoelectric Sensor. In Proceedings of the Smart Structures and Materials 2004: Smart Electronics, MEMS, BioMEMS, and Nanotechnology, International Society for Optics and Photonics, San Diego, CA, USA, 14–18 March 2004; Volume 5389, pp. 377–388.
44. Spencer, S.; Emmons, S.A. Backing Assembly for Use in Z-Mill Type Rolling Mills. WO2009041946A1, 2 April 2009.
45. Cao, Q.; Beden, S.; Beckmann, A. A core reference ontology for steelmaking process knowledge modelling and information management. *Comput. Ind.* **2022**, *135*, 103574. [CrossRef]
46. Brusa, E.; Lemma, L.; Benasciutti, D. Vibration analysis of Sendzimir cold rolling mill and bearing fault detection. *Proc. ImechE Part C J. Mech.Eng. Sci.* **2010**, *224*, 1645–1654. [CrossRef]
47. Rothera, A.; Jelali, M.; Söffkerc, D. A brief review and a first application of time-frequency-based analysis methods for monitoring of strip rolling mills. *J. Process Control.* **2015**, *35*, 65–79. [CrossRef]
48. Kumar, S.; Madhab, G.B. Development of a DSP-Based Motor Health Monitoring System. In Proceedings of the 2006 IEEE International Symposium on Industrial Electronics, Montreal, QC, Canada, 9–13 July 2006; Volume 3, pp. 2373–2376.
49. De Pasquale, G.; Brusa, E.; Soma, A. Capacitive Vibration Energy Harvesting with Resonance Tuning. In Proceedings of the 2009 Symposium on Design, Test, Integration Packaging of MEMS/MOEMS, Rome, Italy, 1–3 April 2009; pp. 280–285.
50. Brusa, E.; Carabelli, S.; Carraro, F.; Tonoli, A. Electromechanical Tuning of Self-Sensing Piezoelectric Transducers. *J. Intell. Mater. Syst. Struct.* **1998**, *9*, 198–209. [CrossRef]
51. Kashyap, R. *Fiber Bragg Gratings*; Academic Press: Cambridge, MA, USA, 2009; ISBN 9780080919911.
52. Yin, S.; Ruffin, P.B.; Yu, F.T.S. *Fiber Optic Sensors*, 2nd ed.; CRC Press: Boca Raton, FL, USA, 2017; ISBN 978-1-315-21943-1.
53. Kreuzer, M. *Strain Measurement with Fiber Bragg Grating Sensors*; HBM Darmstadt S2338-1.0; HBM: Darmstadt, Germany, 2009.
54. Ramakrishnan, M.; Rajan, G.; Semenova, Y.; Farrell, G. Overview of Fiber Optic Sensor Technologies for Strain/Temperature Sensing Applications in Composite Materials. *Sensors* **2016**, *16*, 99. [CrossRef] [PubMed]
55. Yao, K.; Lin, Q.; Jiang, Z.; Zhao, N.; Tian, B.; Shi, P.; Peng, G.-D. Modeling and Analysis of a Combined Stress-Vibration Fiber Bragg Grating Sensor. *Sensors* **2018**, *18*, 743. [CrossRef]
56. Wang, W.; Yu, Y.; Geng, Y.; Li, X. Measurements of Thermo-Optic Coefficient of Standard Single Mode Fiber in Large Temperature Range. In Proceedings of the 2015 International Conference on Optical Instruments and Technology: Optical Sensors and Applications, Beijing, China, 10 August 2015; p. 96200Y. [CrossRef]
57. Roman, M.; Balogun, D.; Zhuang, Y.; Gerald, R.E.; Bartlett, L.; O'Malley, R.J.; Huang, J. A Spatially Distributed Fiber-Optic Temperature Sensor for Applications in the Steel Industry. *Sensors* **2020**, *20*, 3900. [CrossRef]
58. Xu, M.G.; Archambault, J.-L.; Reekie, L.; Dakin, J.P. Discrimination between Strain and Temperature Effects Using Dual-Wavelength Fibre Grating Sensors. *Electron. Lett.* **1994**, *30*, 1085–1087. [CrossRef]
59. Kiniry, J.R. Wavelength Division Multiplexing: Ultra High Speed Fiber Optics. *IEEE Internet Comput.* **1998**, *2*, 13–15. [CrossRef]
60. Available online: https://www.phase-trans.msm.cam.ac.uk/2007/tetra/A/A-Pages/Image0.html (accessed on 3 May 2021).
61. Available online: https://www.koyo.eu/it/media-downloads/catalogo-jtekt-on-line.html (accessed on 3 May 2021).
62. Alian, H.; Konforty, S.; Ben-Simon, U.; Klein, R.; Tur, M.; Bortman, J. Bearing Fault Detection and Fault Size Estimation Using Fiber-Optic Sensors. *Mech. Syst. Signal Processing* **2019**, *120*, 392–407. [CrossRef]
63. Available online: http://www.crsrl.com/steel-mill-and-sendzimir-steel-mill.html (accessed on 3 May 2021).
64. Serdio, F.; Lughofer, E.; Pichler, K.; Buchegger, T.; Efendic, H. Residual-based fault detection using soft computing techniques for condition monitoring at rolling mills. *Inf. Sci.* **2014**, *259*, 304–320. [CrossRef]
65. Chen, J.; Wan, Z.; Pan, J.; Zi, Y.; Wang, Y.; Chen, B.; Sun, H.; Yuan, J.; He, Z. Customized maximal-overlap multiwavelet denoising with data-driven group threshold for condition monitoring of rolling mill drivetrain. *Mech. Syst. Signal Processing* **2016**, *68–69*, 44–67. [CrossRef]
66. Farina, M.; Osto, E.; Perizzato, A.; Piroddi, L.; Scattolini, R. Fault detection and isolation of bearings in a drive reducer of a hot steel rolling mill. *Control. Eng. Pract.* **2015**, *39*, 35–44. [CrossRef]

67. Agliullin, T.; Gubaidullin, R.; Sakhabutdinov, A.; Morozov, O.; Kuznetsov, A.; Ivanov, V. Addressed Fiber Bragg Structures in Load-Sensing Wheel Hub Bearings. *Sensors* **2020**, *20*, 6191. [CrossRef]
68. York, D.; Evensen, N.M.; Martínez, M.L.; De Basabe Delgado, J. Unified Equations for the Slope, Intercept, and Standard Errors of the Best Straight Line. *Am. J. Phys.* **2004**, *72*, 367–375. [CrossRef]
69. İçen, D.; Demirhan, H. Error Measures for Fuzzy Linear Regression: Monte Carlo Simulation Approach. *Appl. Soft Comput.* **2016**, *46*, 104–114. [CrossRef]
70. Bachelor, G.; Brusa, E.; Ferretto, D.; Mitschke, A. Model Based Design of complex aeronautical systems through Digital Twin and Thread concepts. *IEEE Syst. J.* **2020**, *14*, 1568–1579. [CrossRef]
71. Brusa, E.; Ferretto, D.; Calà, A. Integration of Heterogeneous Functional-vs-Physical Simulation within the Industrial System Design Activity. In Proceedings of the 2015 IEEE International Symposium on Systems Engineering (ISSE), Rome, Italy, 28–30 September 2015; pp. 303–310.